Controlling Residual Stress and Suppression of Anomalous Grains in Aluminum Scandium Nitride Films Grown Directly on Silicon

Rossiny Beaucejour, *Member, IEEE*, Volker Roebisch, Abhay Kochhar, *Senior Member, IEEE*, Craig G. Moe, *Member, IEEE*, Michael David Hodge, and Roy H. Olsson III, *Senior Member, IEEE*

***Abstract*— Deposition of Aluminum Scandium Nitride (AlScN) films directly on Silicon at high Sc alloying levels, with controlled stress, and free of anomalous grains (AOGs) is demonstrated using reactive co-sputtering. The average stress and AOG formation consider the Sc alloying range between 20.3 and 36.6 atomic % and for film thicknesses from 400 nm to 1000 nm for 27.3% and 31.7% Sc alloying. The combination of a gradient seed layer and proper process gas mixture is shown to inhibit formation of AOGs in AlScN with up to 36% Sc alloying even when grown directly on Si. It is demonstrated that the total flow can be utilized to control the average film stress across the 20-36% doping range while the process gas mixture primarily impacts the density of AOG formation in the AlScN films. Bulk acoustic wave resonators fabricated from 380 nm and 485 nm thick low stress and AOG free $Al_{0.68}Sc_{0.32}N$ films grown directly on Si demonstrate high frequency operation of 3.6 and 4.8 GHz, high electromechanical coupling >20%, and quality factors in excess of 500. [2021-0252]**

***Index Terms*— Bulk acoustic wave devices, piezoelectric films, piezoelectric resonators, semiconductor defectors, stress control, physical vapor deposition.**

I. Introduction

ADVANCEMENTS in wireless and sensor technology have resulted in increasing demand for piezoelectric MEMS devices in wireless handsets and base stations, automobile technology, health monitoring sensors, and environmental sensors [1]–[4]. Due to its high quality factor (Q), Young's modulus, sound velocity, and low mechanical and dielectric losses, Aluminum Nitride (AlN) is an advantageous resonator material with applications in radio frequency filtering [2], [4], [5]. During processing of AlN films, built in stress and undesired microstructures impact the quality of the film and ultimately the performance of the device. In addition, AlN's low piezoelectric coefficients limit its application, especially when large electromechanical coupling is required such as in wide bandwidth acoustic filters and energy harvesters.

In 2010, it was discovered that alloying AlN with Scandium (Sc) increases its d_{33} piezoelectric coefficient by over 500% and maintains compatibility with post-CMOS integration when deposited below 400° [4]. Further studies demonstrated that high quality and low stress AlScN [6] films possess enhanced electromechanical coupling (k_t^2) above that observed for pure AlN of approximately 7.6% for bulk acoustic wave resonators (BAW) [2] and 1.8% for AlN Lamb wave resonators (LWR) [7] as well as AlScN phase velocities of greater than 8000 m/s [3], [8]. As process parameters and Sc levels are modified to enhance performance, this also impacts the built-in stress in the film. Undesired stress can degrade device performance in thin films. In 2015 Fichtner [6] analyzed stress in AlScN up to 37% Sc concentration deposited on Platinum (Pt) using pulsed DC reactive co-sputtering. Stress was controlled by modifying Ar and N_2 gas mixtures, process pressure, and Sc levels although there was a high density of anomalously oriented grains (AOGs) reported [6]. In 2017 Fichtner [9] reported decreased AOG formation in AlScN materials between 27% and 43% Sc concentration deposited on both Pt and Molybdenum (Mo) electrodes with gas flows of 15 sccm N_2 and 5.3 sccm Ar. Platinum has chemical inertness and is often utilized as a seed electrode for AlScN. Mo is also selected in MEMS processes for improved lattice matching and selective wet etching [9] of the electrode and AlScN. Platinum also has adequate lattice matching but is expensive and is not a standard metal utilized in CMOS processing. Henry [10] found that a Ti, TiN, and AlCu seed reduced anomalous grains in 12.5% single target reactive sputtered AlScN [10]. Bogner and Esteves [7], [11] deposited Aluminum Scandium Nitride using pulsed dc magnetron sputtering up to 20% and 32% Sc alloying respectively. Esteves used Ti, Titanium Nitride (TiN), Aluminum Copper (AlCu), Ti/AlCu, and Ti/TiN/AlCu metal stacks as the seed layers for AlScN growth [7]. Esteves also considered AlScN on an AlN seed, but the Ti/TiN/AlCu more consistently suppressed undesired grains [1]. Bogner [11], [12] used SiN,

Manuscript received 3 December 2021; revised 28 February 2022; accepted 19 March 2022. Date of publication 6 May 2022; date of current version 2 August 2022. This work was funded in part by the NSF CAREER Award (1944248) and in part The Defense Advanced Research Projects Agency (DARPA) Small Business Innovation Research (SBIR) under Award HR0011-21-9-0004. This work was carried out in part at the Singh Center for Nanotechnology at the University of Pennsylvania, a member of the National Nanotechnology Coordinated Infrastructure (NNCI) network, which is supported by the National Science Foundation (Grant No. HR0011-21-9-0004). Subject Editor S. Gong. *(Corresponding author: Roy. H. Olsson III.)*

Rossiny Beaucejour is with the Department of Mechanical Engineering and Applied Mechanics, University of Pennsylvania, Philadelphia, PA 19104 USA (email: rossiny@seas.upenn.edu).

Volker Roebisch is with Evatec AG, 9477 Trübbach, Switzerland.

Abhay Kochhar, Craig G. Moe, and Michael David Hodge are with Akoustis, 9805-A Northcross Center Court, Huntersville, NC 28078 USA.

Roy H. Olsson III is with the Department of Electrical and Systems Engineering, University of Pennsylvania, Philadelphia, PA 19104 USA (e-mail: rolsson@seas.upenn.edu).

Digital Object Identifier 10.1109/JMEMS.2022.3167430

Ti, and Ti/Pt varying seeds layers to decrease undesired grain formation. The 30 nm of Ti and 30 nm of Pt improved suppression of undesired grain growth and exhibited superior electrical performance.

Certain applications in MEMs devices [2], RF resonators [8], and quantum structures [13] desire direct growth of AlScN on Silicon substrates while maintaining both stress control and suppression of anomalous grains. AlScN with low AOG density has been previously demonstrated on <111> FCC metals [1]. Si is a diamond center cubic structure which presents neither hexagonal symmetry nor a close lattice parameter to AlScN, making growth directly on Si more challenging. Compared to studies on Pt, Mo, Al, Ti, and W, these metals all present hexagonal symmetry with a close lattice spacing to AlScN. The poor lattice matching of Si with AlScN results in AlScN films that are more compressive at a given Sc alloying ratio when compared to previously explored AlScN films on FCC metals [6], [11]. The poor lattice match also introduces a higher number of defects that promotes the nucleation of AOGs.

Akiyama [4] used Radio Frequency (RF) magnetron reactive co-sputtering to deposit AlScN directly on n-type Silicon demonstrating a maximum piezoelectric response at 43% Sc concentration. The c-axis orientation degraded significantly between 30% to 40% Sc concentration while undesired cubic phases dominated above 46% Sc. Stress control was not reported by Akiyama [4] and the published results indicate formation of AOGs but the density cannot be determined from the publication. Similarly, Shao et al [3] displayed a low density of AOGs on Pt but significant AOG coverage for thin films directly grown on silicon on the same wafer.

Undesired phases and AOGs reduce piezoelectric coefficients, film orientation, and modify stress. AOGs also render etching of device structures problematic as the AOG regions etch at a much lower rate. When high compressive stress persists, Euler buckling, and inclusions reduce performance in suspended devices. High tensile stress can result in cracking and delamination [1], [10]. Depending on the type of device and the process utilized, the stress will need to stay within a specific range. Thus, independent control of the stress and the piezoelectric properties is important for device performance. We report methods to deposit high quality AlScN films directly on Si with controlled average stress and free of anomalous grains using reactive co-sputtering. We study the average stress and AOG formation for the Sc alloy range between 20.3 and 36.6 atomic % and for film thicknesses from 400 nm to 1000 nm at 27.3% and 31.7% Sc. We demonstrate that a gradient seed layer can be utilized to suppress AOGs when depositing AlScN films directly on Si. We demonstrate that the total flow can be utilized to control the average film stress while the process gas mixture impacts the density of AOGs in the film. Finally, we demonstrate the utility of our growth processes by realizing high electromechanical coupling (>20%) and high figure-of-merit bulk acoustic wave (BAW) resonators from low stress 380 nm and 485 nm thick $Al_{0.68}Sc_{0.32}N$ materials grown directly on Si.

TABLE I
SPUTTER DEPOSITION PARAMETERS FOR ALSCN SCANDIUM CONCENTRATION EXPERIMENT

Process Parameter	*Value*
Temperature	*350 °C*
Sputter Power Al Cathode	*1000 W*
Sputter Power Sc Cathode	*300-655 W*
DC Pulsing Frequency	*150 kHz*
N_2 Flow	*20 sccm*
Ar Flow	*0 sccm*
Film Thickness	*500 nm*
Base Pressure	*< $3x10^{-7}$ mbar*

TABLE II
EQUIVALENT SCANDIUM CATHODE POWER TO SCANDIUM CONCENTRATIONS MEASURED BY EDS

Sc (W)	*300*	*400*	*450*	*555*	*605*	*655*
Sc (%)	*20.3*	*24.9*	*27.3*	*31.7*	*34.5*	*36.6*

II. EXPERIMENTATION DETAILS

A. AlScN Sputtering Process Parameters and Metrology Methods

AlScN is deposited directly onto 100 mm p-type Si wafers for stress optimization and 150 mm p-type Si wafers for BAW device fabrication using an Evatec pulsed DC reactive co-sputtering system at various Sc powers and sputtering conditions, summarized in Tables I-V. Depositions on the 100 mm wafers were performed using a 150 mm pocket wafer. The scandium cathode power, Al cathode power, temperature, gas flow, process gas mixture, and substrate-to-target distance all impact the Sc level, growth rate, average stress, and crystallinity of the resulting film. The Aluminum power is held constant through these experiments while the Sc cathode power is modified to control the Sc alloying in the resulting films [14]. To determine the impact on the Sc alloying ratio of the Sc cathode power, samples using a Sc cathode power of 450, 555, 605, and 655 W were produced while holding the while holding the Al cathode power constant at 1000 W [14]. Both targets were 100 mm in diameter. The scandium concentration was then measured for each sample using energy dispersive X-ray spectroscopy (EDS) in a scanning electron microscope (SEM) resulting in Sc concentrations of 27.3 (450 W), 31.7 (555 W), 34.4 (605 W), and 36.6 (655 W). An epitaxial $Al_{52}Sc_{48}N$ material, where the composition was previously verified using Rutherford Backscattering Spectrometry (RBS), was used as a reference sample for the k-factor analysis during the measurement of these samples [15]. When utilizing a reference sample, SEM/EDS measurements have been shown to be highly accurate with less than 2% relative error [16]. The SEM/EDS measurements of these samples were then used to determine the Sc cathode power required

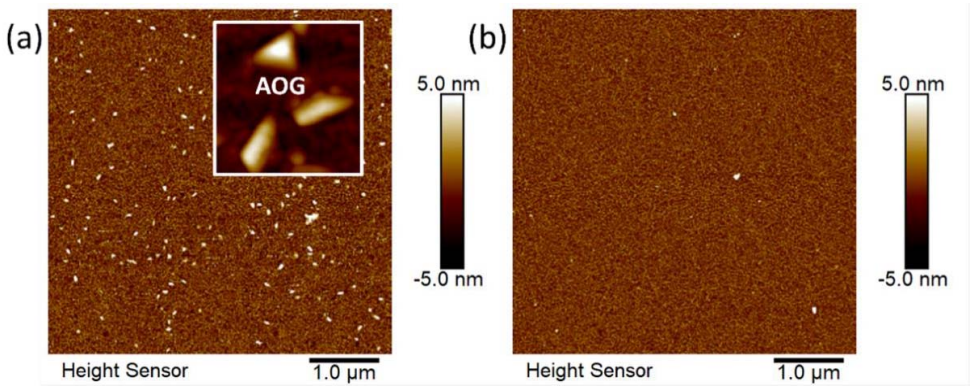

Fig. 1. AFM micrographs of 500nm PVD deposited $Al_{0.68}Sc_{0.32}N$ films **(a)** with no gradient layer, no Argon gas and 20 sccm Nitrogen gas and **(b)** with a gradient layer with no Argon gas and 25 sccm Nitrogen gas.

to produce samples of varying Sc alloying levels. To aid in the suppression of AOGs, a 15 nm AlN seed and a 35 nm gradient seed layer are utilized. The gradient seed layer, where the Sc concentration is linearly graded from 0% Sc alloying to the final Sc concentration over a thickness of 35 nm, sits on top of the AlN seed. The gradient seed layer is formed by linearly increasing the Sc cathode power with time from 0 W to the power corresponding to the desired final alloying level reported in Table II. Atomic Force Microscope (AFM) micrographs in Figure 1 display how this seed layer suppresses the formation of AOGs in Figure 1(b) when compared to unseeded materials in Figure 1(a). The final thickness of the film is measured using a Woollam Ellipsometer. The film orientation is assessed using the rocking curve full width half maximum (FWHM) from an ω-scan in a Rigaku X-Ray diffraction (XRD) machine with Cu-Kα source and the roughness and surface structure are measured using a Bruker AFM. The average stress is measured using a Tencor (Keep Looking Ahead) KLA stress profilometer. The average film stress is computed by first measuring the wafer's radius of curvature before and after deposition using a profilometer then subsequently calculated using Stoney's equation [6], [17], [18]. This method was previously shown to be repeatable within $\pm$20 MPa [19].

III. Results and Discussion

A. Scandium Concentration

The DC power provided to the Scandium (Sc) cathode accelerates more plasma towards the target, releases more Sc ions into the environment, and raises the percentage (in atomic %) of Sc in Aluminum Scandium Nitride films. The $Al_{0.68}Sc_{0.32}N$ materials were sputtered under the conditions shown in Table I. Table II provides the corresponding Scandium cathode power and its resulting Sc percentage for 500 nm films deposited with gas flows of 0 sccm Ar and 20 sccm N_2. A power of 300 W provided 20.3% Sc alloyed AlScN, while increasing the power to 655 W increased the content to 36.6%. In Figure 2(a), large average compressive stresses arise with higher percentages of Sc. These compressive stresses can lead to buckling in MEMS plates and clamp-clamp beams. The average stress decreases at a near linear rate with increasing Sc content.

TABLE III
Sputter Deposition Parameters for AlScN Gas Flow and Total Gas Flow Experiment

Process Parameter	*Value*
Temperature	*350 °C*
Sputter Power Al Cathode	*1000 W*
Sputter Power Sc Cathode	*555 W*
DC Pulsing Frequency	*150 kHz*
N_2 Flow	*15-30 sccm*
Ar Flow	*0-10 sccm*
Film Thickness	*500 nm*
Base Pressure	*< $3x10^{-7}$ mbar*

Increases in Sc concentration have been shown to increase the piezoelectric coefficients. This study reveals that additional processing parameters are required to reduce the compressive stress developed if highly Sc alloyed materials are to be utilized in MEMS devices.

Figures 2(a) and 3 show the trends in the orientation and structure of the films. The full-width half-maximum (FWHM) of the film is decreasing with increasing Scandium alloying which demonstrates the ability to deposit AlScN films with high c-axis orientation required for large piezoelectricity. The 002 peak in the XRD 2-theta plot of Figure 3 increases slightly from 36° with increased Sc alloying, indicting a change in the distance between the atomic planes in the crystal using Braggs law. The results provide corroborating evidence of higher in-plane compressive stress being imparted into materials with high amounts of Sc incorporation.

B. Process Gas Flow Rate and Process Gas Mixture

Figure 2(c) shows the resulting average film stress of $Al_{0.68}Sc_{0.32}N$ as the total gas flow is increased from 20 sccm to 40 sccm for a 500 nm thick film with depositions parameters provided in Table III. In Figure 2(c) different gas mixtures are utilized. The AlScN film becomes more tensile with increasing total process gas flow. The average stress is a strong function of the total gas flow but varies minimally based on the ratio of

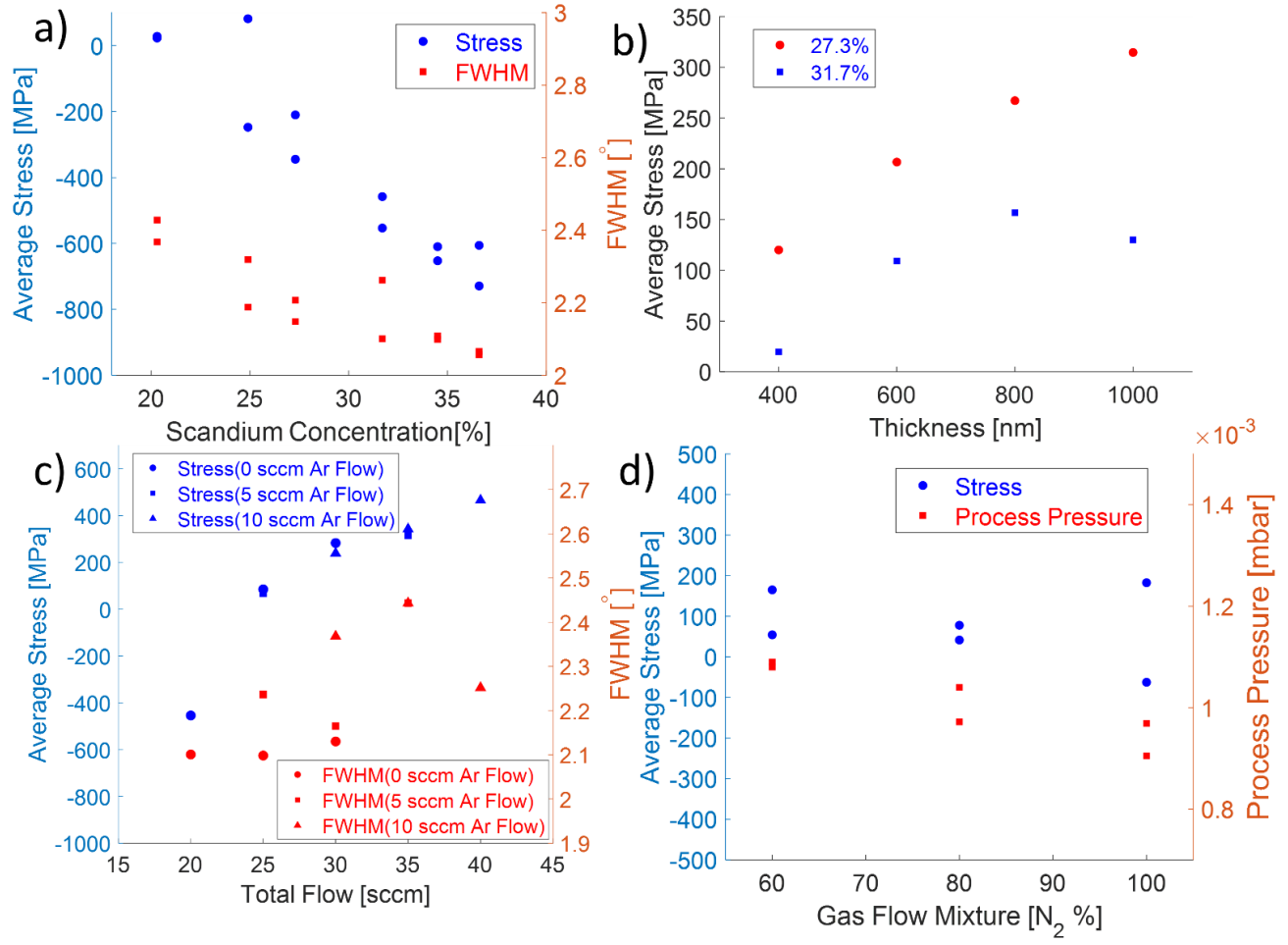

Fig. 2. Study of average stress and full width half max (FWHM) for $Al_{1-x}Sc_xN$ films for **(a)** Scandium concentrations between 20.3% to 36.6% at gas flows of 0 sccm Ar, 20 sccm N_2, and 500 nm film thickness **(b)** Varying film thicknesses between 400 nm and 1000 nm deposited at 27.3% and 31.7% Scandium, 0 sccm Ar, and 25 sccm N_2 **(c)** Total flow from 20 to 40 sccm at 31.7% Scandium, 500 nm film thickness, varying gas mixtures of 0, 5, and 10 sccm Ar and **(d)** Increasing concentrations of N_2 at a constant 25 sccm total flow at 31.7% Scandium and 500 nm film thickness. The corresponding process pressure for the flow conditions is also shown.

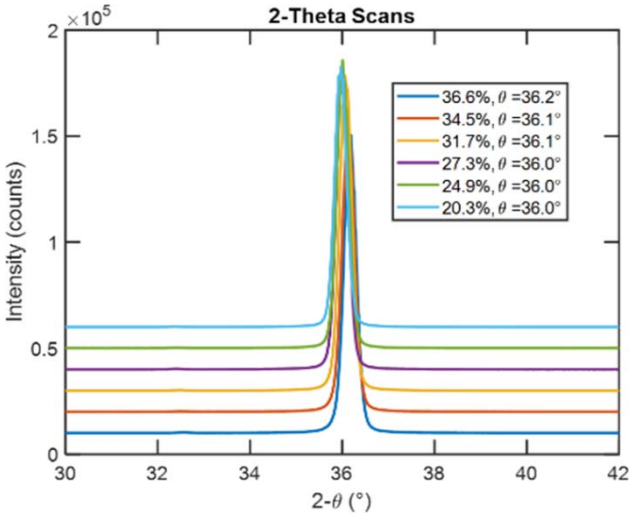

Fig. 3. XRD plots of AlScN at Sc concentrations between 20.3-36.6%. 1000 counts have been added to the intensity of each sequential plot for visualization.

Ar to N_2 used for the process gasses, as shown in Figure 2(c). Figure 2(d) provides a plot of average stress at a constant 25 sccm total flow while the ratio of the constituent Ar and N_2 gasses are varied. As the N_2 concentration increases, the resulting average film stress remains nearly constant. These experiments indicate the total flow (or process pressure) is the critical parameter in controlling average stress. Nitrogen concentrations can be increased to maintain the same level of average stress without the need to flow Ar gases into the chamber. Higher process gas, total flow, and an increase in Ar flow degraded the film properties as indicated by the increased FWHM in Figure 2(c) and the AOG formation seen in Figure 4. A constant flow of 25 sccm produces the slightly tensile average stresses desired in many MEMS devices and processes for 500 nm thick $Al_{0.68}Sc_{0.32}N$. Varying the total process gas flow also alters the surface structure of the AlScN. While the process gas mixture has minimal effect on the residual average film stress, it has a profound impact on the AOG formation.

The AFM images in Figure 4 show the increased surface roughness and formation of undesired grains that can occur at increased process pressures. As Ar gas flow is increased, a higher AOG density is observed on the film surface leading to a higher surface roughness. High surface roughness can scatter acoustic waves propagating in resonant MEMS devices which lowers their quality factor.

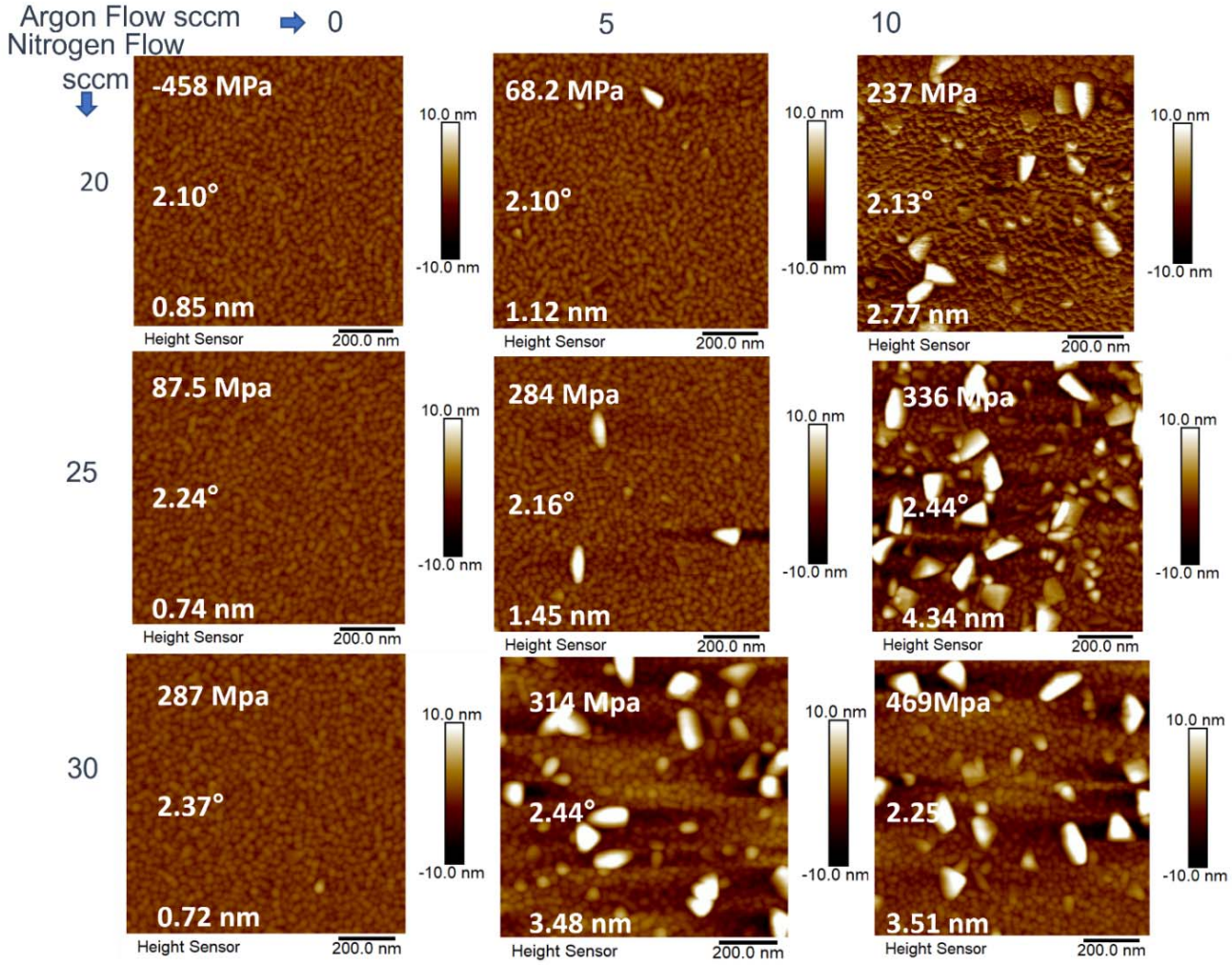

Fig. 4. 2D AFM images of $1\mu m \times 1\mu m$ area scans for AlScN with ranges of Nitrogen and Argon flows from 20-30 sccm and 0-10 sccm, respectively. Bright triangular features are anomalously oriented grain growth (AOG), average in-plane film stress is provided in the top left corner of each image, FWHM is provided on the middle left, and the surface roughness of the film is provided in the bottom left corner. These 500 nm films were sputtered at 350°C and cathode powers of 555 W Sc (31.7% Sc) and 1000 W Al.

TABLE IV
SPUTTER DEPOSITION PARAMETERS FOR ALSCN FILM THICKNESS EXPERIMENT

Process Parameter	*Value*
Temperature	*350 °C*
Sputter Power Al Cathode	*1000 W*
Sputter Power Sc Cathode	*450 W and 555 W*
DC Pulsing Frequency	*150 kHz*
N_2 Flow	*25 sccm*
Ar Flow	*0 sccm*
Film Thickness	*0.4 um, 0.6 um, 0.8 um, and 1 um*
Base Pressure	*< 3x10^{-7} mbar*

TABLE V
SPUTTER DEPOSITION PARAMETERS FOR ALSCN XBAW DEVICE FABRICATION PROCESS

Process Parameter	*Value*
Temperature	*350 °C*
Sputter Power Al Cathode	*1000 W*
Sputter Power Sc Cathode	*555 W*
DC Pulsing Frequency	*150 kHz*
N_2 Flow	*25 sccm*
Ar Flow	*0 sccm*
Base Pressure	*< 3x10^{-7} mbar*

Furthermore, anomalously oriented grains do not contribute to the piezoelectric response [2] but contribute to the mass, stiffness, and capacitance of the material, thereby decreasing the electromechanical coupling. When Ar is removed from the process gas mixture, the roughness is observed to decrease and smooth films free of AOGs can be formed. Depositions free of Ar process gas were found to suppress AOG formation and allow process gas flows up to 30 sccm N_2 to tailor the residual average film stress in $Al_{0.68}Sc_{0.32}N$ over the range from −458 to +287 MPa.

TABLE VI

DEVICE PARAMETERS FOR BAW RESONATORS FORMED FROM THE 380 NM AND 485 NM $AL_{0.68}Sc_{0.32}N$ MATERIALS IN THE AKOUSTIS XBAW PROCESS AND COMPARISON TO STATE-OF-THE-ART

Sc (%)	f_s (GHz)	f_p (GHz)	k_{eff}^2 (%)	k_t^2 (%)	Q_s	Q_p	thickness (nm)	FOM	FOM•f_p•10^{-9}	Source
20	1.79	1.9	11.2	15.6	---	890	890	113	215	Bogner [12]
20	4.09	4.29	9.1	12.4	---	210	400	21	90	Bogner [12]
28	3.33	3.56	12.5	17.6	530	831	762	119	424	Moe [8]
30	2.93	3.17	14.6	21.0	328.5	---	900	56*	178	Wang [20]
32	3.61	3.94	16.0	23.6	776	574	485	110	433	This work
32	4.8	5.23	15.8	23.1	545	630	380	118	617	This work

*FOM calculated using reported Q_s

AlScN films at thicknesses ranging from 400 nm to 1000 nm and Sc alloys at 27.3% and 31.7% were sputter deposited using 0 sccm Ar and 25 sccm N_2 process gases on 100 mm wafers. Table IV provides depositions parameters used for this study. At larger film thickness, tensile stress increased in the AlScN films for all Sc concentrations. The 25 sccm N_2 gas flow was optimized for the 31.7% Sc alloy, but a slightly lower total flow will achieve the equivalent average stress for the 27.3% alloys. The trend in Figure 2(b) confirms increasing average stress with an increase in film thickness and indicates a stress gradient from compressive to tensile through the thickness of the AlScN materials. Deposition processes to suppress this stress gradient are the subject of on-going research.

C. Device Realization and Performance

High quality $Al_{0.68}Sc_{0.32}N$ films of 380 nm and 485 nm thicknesses were deposited directly on 150 mm diameter Si wafers and were subsequently integrated into the Akoustis XBAW process to realize high performance bulk acoustic wave (BAW) resonators. The Akoustis XBAW process can integrate films grown directly on Si into BAW resonators with top and bottom electrodes as previously demonstrated by Moe [8] and Kim [21]. The $Al_{0.68}Sc_{0.32}N$ materials were sputtered under the conditions shown in Table V. The films were free of AOGs and exhibited average residual stress levels of −178 MPa and −142 MPa for the 380 nm and 485 nm thick films respectfully. The difference in the average stress levels observed between the 100 mm and 150 mm diameter wafers arises from the more compressive AlScN stress observed near the edges of the 150 mm wafers. The 100 mm diameter wafers used for the stress optimization studies in Figures 1-4 were deposited in a 150 mm pocket wafer and have stress values similar to the center 100 mm of a 150 mm diameter wafer. The wafers exhibit a stress distribution of more tensile in the wafer center to more compressive at the wafer edges that results in a more compressive average film stress for the 150 mm wafers.

To form BAW resonators, the 380 nm thick AlScN materials were integrated with 99 nm thick top and 90 nm thick bottom Molybdenum electrodes using the Akoustis XBAW process.

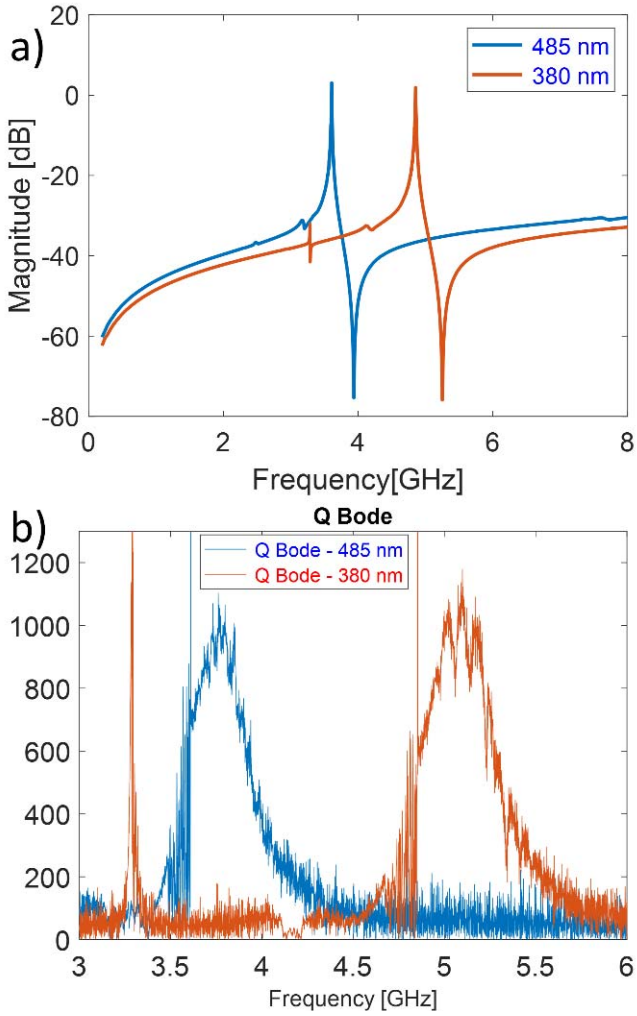

Fig. 5. (a) Y-Parameters of resonators with Akoustis XBAW process using 380 nm and 485 nm deposited with 0 sccm Ar and 25 sccm N_2 and (b) Bode Q plot for 380 nm and 485 nm.

Similarly, the 485 nm AlScN materials were integrated with 143 nm thick top and 120 nm thick bottom Molybdenum electrodes. Figure 5 shows (a) the admittance plots and (b) the

Bode Q values of the resonators fabricated from the 380 and 485 nm $Al_{0.68}Sc_{0.32}N$ films. The 485 nm thick $Al_{0.68}Sc_{0.32}N$ films resulted in a BAW resonant frequency of 3.61 GHz, a $k_t^2 = 23.6\%$ and series (Q_s) and parallel (Q_p) quality factors of 776 and 574. The k_t^2 was determined by measuring the series and parallel resonant peaks, f_s and f_p, according to equations 1 and 2.

$$k_{eff}^2 = \frac{f_p^2 - f_s^2}{f_p^2} \quad \text{(Eq. 1)}$$

$$k_t^2 = \frac{\pi^2}{8}\left(\frac{k_{eff}^2}{1 - k_{eff}^2}\right) \quad \text{(Eq. 2)}$$

The figure-of-merit for the 3.94 GHz resonator was calculated to be 110 from equation 3.

$$FOM = \frac{k_{eff}^2 Q_p}{1 - k_{eff}^2} \quad \text{(Eq. 3)}$$

The 380 nm thick $Al_{0.68}Sc_{0.32}N$ films resulted in a BAW series resonant frequency of 4.8 GHz, a $k_t^2 = 23.1\%$ and series (Q_s) and parallel (Q_p) quality factors of 545 and 630. Table VI compares the performance to state-of-the-art high coupling BAW resonators from the literature, where a compelling combination of high coupling, high quality factor, and high frequency operation is demonstrated.

IV. Conclusion

This study reported on stress control and anomalously oriented grain suppression in AlScN thin films deposited directly on Si using sputter deposition. Methods to maintain a high degree of crystallinity across the Sc doping range, to control average film stress, and to limit formation of undesired grains were studied by utilizing a gradient seed layer, tuning the total flow, and controlling constituent gas species. The films were optimized to control stress, suppress AOGs, and increase piezoelectric coefficient via aggressive Sc alloying. The resulting films exhibit a high degree of crystallinity and low surface roughness and are therefore promising for next generation MEMS devices. The exceptional piezoelectric properties, high film quality, low surface roughness, and low stress were confirmed via the demonstration of high coupling and high FOM BAW resonators operating at 3.61 and 4.8 GHz.

Acknowledgment

The views and conclusions contained in this document are those of the authors and should not be interpreted as representing the official policies, either expressed or implied, of the U.S. Government.

Conflicts of Interest

The authors have no conflicts to disclose.

Data Availability

The data that support the findings of this study are available from the corresponding author upon reasonable request.

References

[1] G. Esteves, M. Berg, K. D. Wrasman, M. D. Henry, B. A. Griffin, and E. A. Douglas, "CMOS compatible metal stacks for suppression of secondary grains in $Sc_{0.125}Al_{0.875}N$," *J. Vac. Sci. Technol. A, Vac. Surf. Films*, vol. 37, no. 2, Mar. 2019, Art. no. 021511.

[2] R. H. Olsson, Z. Tang, and M. D'Agati, "Doping of aluminum nitride and the impact on thin film piezoelectric and ferroelectric device performance," in *Proc. IEEE Custom Integr. Circuits Conf. (CICC)*, Mar. 2020, pp. 1–6.

[3] S. Shao, Z. Luo, and T. Wu, "High figure-of-merit Lamb wave resonators based on $Al_{0.7}Sc_{0.3}N$ thin film," *IEEE Electron Device Lett.*, vol. 42, no. 9, pp. 1378–1381, Sep. 2021.

[4] M. Akiyama, T. Kamohara, K. Kano, A. Teshigahara, Y. Takeuchi, and N. Kawahara, "Enhancement of piezoelectric response in scandium aluminum nitride alloy thin films prepared by dual reactive cosputtering," *Adv. Mater.*, vol. 21, no. 5, pp. 593–596, 2008.

[5] K. Kusaka, D. Taniguchi, T. Hanabusa, and K. Tominaga, "Effect of sputtering gas pressure and nitrogen concentration on crystal orientation and residual stress in sputtered AlN films," *Vacuum*, vol. 66, nos. 3–4, pp. 441–446, 2002.

[6] S. Fichtner, T. Reimer, S. Chemnitz, F. Lofink, and B. Wagner, "Stress controlled pulsed direct current co-sputtered $Al_{1-x}Sc_xN$ as piezoelectric phase for micromechanical sensor applications," *APL Mater.*, vol. 3, no. 11, Nov. 2015, Art. no. 116102.

[7] G. Esteves *et al.*, "$Al_{0.68}Sc_{0.32}N$ Lamb wave resonators with electromechanical coupling coefficients near 10.28%," *Appl. Phys. Lett.*, vol. 118, no. 17, Apr. 2021, Art. no. 171902.

[8] C. Moe *et al.*, "Highly doped AlScN 3.5 GHz XBAW resonators with 16% k2eff for 5G RF filter applications," in *Proc. IEEE Int. Ultrason. Symp. (IUS)*, Sep. 2020, pp. 1–4.

[9] S. Fichtner *et al.*, "Identifying and overcoming the interface originating c-axis instability in highly Sc enhanced AlN for piezoelectric microelectromechanical systems," *J. Appl. Phys.*, vol. 122, no. 3, Jul. 2017, Art. no. 035301.

[10] M. D. Henry, T. R. Young, E. A. Douglas, and B. A. Griffin, "Reactive sputter deposition of piezoelectric $Sc_{0.12}Al_{0.88}N$ for contour mode resonators," *J. Vac. Sci. Technol. B, Nanotechnol. Microelectron., Mater., Process., Meas., Phenomena*, vol. 36, no. 3, May 2018, Art. no. 03E104.

[11] A. Bogner *et al.*, "Impact of high Sc content on crystal morphology and RF performance of sputtered $Al_{1-x}Sc_xN$ SMR BAW," in *Proc. IEEE Int. Ultrason. Symp. (IUS)*, Oct. 2019, pp. 706–709.

[12] A. Bogner *et al.*, "Enhanced piezoelectric $Al_{1-x}Sc_xN$ RF-MEMS resonators for sub-6 GHz RF-filter applications: Design, fabrication and characterization," in *Proc. IEEE 33rd Int. Conf. Micro Electro Mech. Syst. (MEMS)*, 2020, pp. 1258–1261, doi: 10.1109/MEMS46641.2020.9056296.

[13] G. S. MacCabe *et al.*, "Nano-acoustic resonator with ultralong phonon lifetime," *Science*, vol. 370, no. 6518, pp. 840–843, Nov. 2020.

[14] D. Wang *et al.*, "Ferroelectric c-axis textured aluminum scandium nitride thin films of 100 nm thickness," in *Proc. Joint Conf. IEEE Int. Freq. Control Symp. Int. Symp. Appl. Ferroelectr. (IFCS-ISAF)*, Jul. 2020, pp. 1–4.

[15] B. Fultz and J. M. Howe, *Transmission Electron Microscopy and Diffractometry of Materials*. Berlin, Germany: Springer, 2012.

[16] D. E. Newbury and N. W. Ritchie, "Is scanning electron microscopy/energy dispersive X-ray spectrometry (SEM/EDS) quantitative?" *Scanning*, vol. 35, no. 3, pp. 141–168, 2013.

[17] M.-A. Dubois and P. Muralt, "Stress and piezoelectric properties of aluminum nitride thin films deposited onto metal electrodes by pulsed direct current reactive sputtering," *J. Appl. Phys.*, vol. 89, no. 11, pp. 6389–6395, Jun. 2001.

[18] V. K. Khanna, *Flexible Electronics*, vol. 2. Bristol, U.K.: IOP Publishing, 2019.

[19] D. Wang *et al.*, "Sub-microsecond polarization switching in (Al,Sc)N ferroelectric capacitors grown on complementary metal–oxide–semiconductor-compatible aluminum electrodes," *Phys. Status Solidi, Rapid Res. Lett.*, vol. 15, no. 5, 2021, Art. no. 2000575.

[20] J. Wang, M. Park, S. Mertin, T. Pensala, F. Ayazi, and A. Ansari, "A film bulk acoustic resonator based on ferroelectric aluminum scandium nitride films," *J. Microelectromech. Syst.*, vol. 29, no. 5, pp. 741–747, 2020.

[21] D. H. Kim, M. Winters, R. Vetury, and J. B. Shealy, "Piezoelectric acoustic resonator manufactured with piezoelectric thin film transfer process," U.S. Patent 10 355 659, Jul. 16, 2019.

Rossiny Beaucejour (Member, IEEE) received the B.S. degree in mechanical engineering from the University of Delaware, the master's degree in materials science and engineering from the University of Maryland, College Park, and the M.S. degree in mechanical engineering and applied mechanics from the University of Pennsylvania (UPENN), where he is currently pursuing the Ph.D. degree in mechanical engineering and applied mechanics. He was a McNair Scholar with the University of Delaware. He worked at Northrop Grumman as a Materials Process Engineer and Microelectronics Packaging Engineering for over four years, before joining UPENN. He is a member of ASME and NSBE.

Volker Roebisch received the B.Sc. and M.Sc. degrees in material science from the University of Kiel, Germany, in 2010 and 2012, respectively. While working with the Research Group Inorganic Functional Materials under the supervision of Prof. E. Quandt with the University of Kiel, his research interests include shape-memory alloys, exchange-biased soft-magnetic multilayers, and piezoelectric layers for magnetoelectric sensing. During his studies and research work, he has gained more than ten years of experience with PVD methods and device fabrication. In his current position as a Process Engineer at Evatec AG, Switzerland, his work focuses on piezoelectric materials.

Abhay Kochhar (Senior Member, IEEE) received the B.E. degree from Nagpur University, India, the M.Tech. degree from VNIT Nagpur, India, and the Ph.D. degree from Tohoku University, Japan. From October 2013 to September 2015, he worked as a Post-Doctoral Research Fellow with WPI-AIMR, Tohoku University. From October 2015 to September 2016, he was a Post-Doctoral Research Associate and from October 2016 to April 2019, he was a Research Scientist, both with the ECE Department, Carnegie Mellon University, Pittsburgh, PA, USA. Since May 2019, he has been working at Akoustis Technologies Inc., Huntersville, NC, USA, where he is currently a Staff Device Engineer. He was awarded Japanese Government (MEXT) Scholarship from 2010 to 2013. He has won the Best Paper Award at IEEE International Ultrasonic Symposium in 2012. His research interests include microfabrication, hetero-integrated systems, and piezoelectric materials for timing and filter applications.

Craig G. Moe (Member, IEEE) received the B.S. degree in applied science from the University of North Carolina, Chapel Hill, in 1998, and the Ph.D. degree in materials from the University of California at Santa Barbara, Santa Barbara, in 2007. He was a Post-Doctoral Researcher with the Army Research Laboratory, Adelphi, MD, USA, from 2007 to 2012, working on UVC optoelectronics. He joined Akoustis Inc., in 2017, where he is currently the Director of materials responsible for piezoelectric AlN and AlScN thin film development for the company's bulk acoustic wave RF filter products. He has authored or coauthored over 30 technical publications and has been awarded 11 patents related to aluminum nitride-based alloys and devices.

Michael David Hodge received the B.S. degree in electrical and computer engineering from North Carolina State University in 2000 and the M.S. and Ph.D. degrees in electrical engineering from the University of North Carolina at Charlotte in 2007 and 2014, respectively. He joined Akoustis Inc., in 2015. He has contributed in multiple roles, including BAW device technology development, modeling, and design of BAW RF filters for defense and commercial wireless applications. Previously, he worked at RF Micro Devices and later Qorvo designing AlGaN/GaN HEMT devices for high power defense applications.

Roy (Troy) H. Olsson III (Senior Member, IEEE) received the Ph.D. degree in electrical engineering from the University of Michigan, Ann Arbor, in 2004. He is currently an Assistant Professor with the Department of Electrical and Systems Engineering, University of Pennsylvania. His research interests include materials, devices, and architectures for low-power processing of wireless, sensor, and biological signals. Prior to joining Penn, he was a Program Manager with the DARPA Microsystems Technology Office (MTO), where he led multiple programs in the areas of low energy sensing and communications. From 2004 to 2014, he was a Principal Electronics Engineer with the MEMS Technologies Department, Sandia National Laboratories, where he established research efforts in piezoelectric microdevices for processing of RF, inertial and optical signals. His graduate research was in the areas of low-power electronics and sensor arrays for interfacing with the central nervous systems. He has authored more than 100 technical journals and conference papers and holds 32 patents in the areas of microelectronics and microsystems. In 2011, he was awarded a Research and Development 100 Award for his work on Microresonator Filters and Frequency References. He was named the 2017 DARPA Program Manager of the year. He was a recipient of the NSF Career Award in 2019.